Nanoscale

Accepted Manuscript

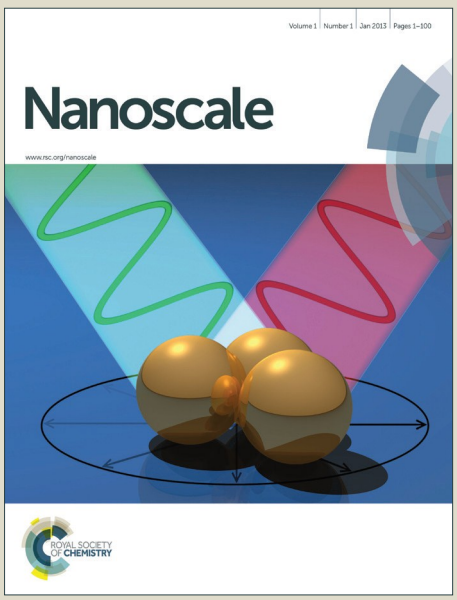

ROYAL SOCIETY OF CHEMISTRY

www.rsc.org/nanoscale

Nanoscale

COMMUNICATION

One-pot one-cluster synthesis of fluorescent and bio-compatible Ag_{14} nanoclusters for cancer cell imaging

Received 00th January 20xx,
Accepted 00th January 20xx

DOI: 10.1039/x0xx00000x

www.rsc.org/

Jie Yang,[a,b] Nan Xia,[a] Xinan Wang,[c] Xianhu Liu,[d] An Xu,[c] Zhikun Wu*,[a], Zhixun Luo*,[d c]

Small-molecule-protected silver nanoclusters have smaller hydrodynamic diameter thus may hold greater potential in biomedicine application compared with same core-sized, macromolecule (i.e. DNA)-protected silver nanoclusters. However, the live cell imaging labeled by small-molecule-protected silver nanoclusters was not reported until now, and the synthesis and atom-precise characterization of silver nanoclusters are challenging for a long time. We develop a one-pot one-cluster synthesis method to prepare silver nanoclusters capped with GSH which is bio-compatible. The as-prepared silver nanoclusters are identified to be $Ag_{14}(SG)_{11}$ (abbreviated as Ag_{14}, SG: glutathione) by isotope-resolvable ESI-MS. The structure is probed by 1D NMR spectroscopy together with 2D COSY and HSQC. This cluster species is fluorescent and the fluorescence quantum yield is solvent-dependent. Very importantly, Ag_{14} was successfully applied to label lung cancer cells (A549) for imaging, and this work represents the first attempt to image live cells with small-molecule-protected silver nanoclusters. Furthermore, it is revealled that the Ag_{14} nanoclusters exhibit lower cytotoxicity compared with some other silver species (including silver salt, silver complex and large silver nanoparticles), and the explanation is also provided. The comparisons of silver nanoclusters to state-of-the-art labeling materials in terms of cytoxicity and photobleaching lifetime were also conducted.

Noble-metal clusters have attracted great interest not only for fundamental science studies but also for technological explorations due to their unique physicochemical properties bridging the gap between those of atoms (also small molecules) and of nanomaterials/nanocrystals.[1] Among the noble metals, gold clusters have been extensively studied primarily due to their relatively facile preparation. Since the pioneering work of Brust et al in 1994, various synthesis methods have been developed, and a range of different sized Au_n thiolate clusters such as Au_{19},[2] Au_{24},[3] Au_{25},[4] Au_{36},[5] Au_{38},[6] Au_{55},[7] Au_{102}[8] and Au_{144}[9] have been successfully synthesized and fully characterized. Although a breakthrough on Ag_{44} structure was made recently,[10] the research on silver nanoclusters obviously lags behind that of gold nanoclusters mainly due to the synthesis difficulty and unstability of silver nanoclusters. By far only a few mono-thiolated silver nanoclusters including Ag_7,[11-13] Ag_8,[12,13] Ag_9,[14] Ag_{16},[15] Ag_{32},[16a,b] Ag_{35},[16c] and Ag_{44}[10,17] were synthesized and characterized by high-resolution mass spectrometry. Overall, the synthesis and precise composition determination of silver nanoclusters still remain a challenge by far, largely hindering the recognized applications[18] in biomedicine and live cell imaging which have attracted reasonable research interest in recent years.[19]

Cell imaging labeled with small-molecule-protected silver nanoclusters has not been reported to our best knowledge. Due to smaller diameter (beneficial to renal clearance,[1e,20] cell penetration, *etc.*), and other merits (easier surface modification, well-defined composition and structure, *etc.*), small-molecule-protected Ag clusters bear some advantages over the macromolecule-protected ones. Also considering that organic fluorophores are prone to photobleaching and fluorescent semiconductor quantum dots are generally made of toxic elements like Cd and Pb, developing small-molecule-protected metal nanoclusters as imaging material is of great importance.[21] In this work, by subtle tuning of reaction parameters we have successfully synthesized a silver nanocluster composed of fourteen silver atoms and eleven glutathionate ligands (abbreviated as Ag_{14}), in a one-pot one-cluster fashion.[10] The composition of the as-prepared monodisperse nanocluster was precisely identified by high-resolution mass spectrometry combined with other analyses. The structure is probed by 1D NMR together with 2D COSY and

[a] *Key Laboratory of Materials Physics, Anhui Key Laboratory of Nanomaterials and Nanotechnology, Institute of Solid State Physics, Chinese Academy of Sciences (CAS), Hefei, 230031, R. P. China. E-mail: zkwu@issp.ac.cn.*
[b] *Department of Chemistry, University of Science and Technology of China, Hefei, 230026, R. P. China.*
[c] *Key Laboratory of Ion Beam Bioengineering, Institute of Technical Biology and Agriculture Engineering, Chinese Academy of Sciences (CAS), Hefei, 230031, R. P. China.*
[d] *State key Laboratory for structural chemistry of unstable and stable species, Institute of Chemistry, Chinese Academy of Sciences (CAS), Beijing, 100190, R. P. China. E-mail: zxluo@iccas.ac.cn.*
† Electronic Supplementary Information (ESI) available: See DOI: 10.1039/x0xx00000x

HSQC. Further, Ag_{14} is successfully applied to label lung cancer cells (A549) for imaging, and this work represents the first attempt to image live cells (as well as cytotoxicity investigations) with small-molecule-protected silver nanoclusters. A comparison of Ag_{14} to some other silver species, quantum dots, organic fluorophores in terms of cytoxicity and photobleaching lifetime were also conducted.

It is known that thiolates play an important role in protecting silver nanoclusters. For instances, meso-2,3-dimercaptosuccinic acid (DMSA),[11a] mercaptosuccinic acid,[12] glutathione (GSH)[16] and 4-mercaptobenzoic acid[10] have been utilized to synthesize stable silver nanoclusters. Among the investigated ligands, glutathione attracts considerable interest due to the following advantages. i) It is water-soluble and bio-compatible. ii) It is bio-active and actually a widely used drug for anti-oxidation, anti-ageing and integrate detoxification. iii) It can impart fluorescence to metal nanoclusters although the ligand itself is of no fluorescence.[22] iv) It is a multidendate ligand with functional groups such as –COOH and $–NH_2$. These advantages are very important for biomedical applications. For instances, the bio-compatibility is fundamental for biomedical consideration,[1e] the imparted fluorescence can be considered for potential bio-imaging, and the additional functional groups such as –COOH and $–NH_2$ can be covalently bonded with some drug molecules for disease therapy. Therefore, it is a reasonable choice to employ glutathione as the protecting ligand to synthesize fluorescent silver nanoclusters.

Besides, a proper choice of the reaction medium is also a key for the successful synthesis of Ag_{14} nanoclusters, *i.e.*, the reaction is solvent-sensitive, and the composition of the product depends on the solvent. In all of the investigated organic solvents (including methanol, ethanol, N,N-dimethylformamide (DMF), THF, *etc.*), monodisperse Ag_{14} nanoclusters were not obtained due to the poor solubility of glutathione in those non-aqueous medium. We found that water is a good solvent medium for the synthesis resulting in high yield of Ag_{14} nanoclusters. The synthesis procedure was carried out in water without avoiding light and air, and the procedure involved three steps (see details in the Supporting Information). First, silver salt ($AgNO_3$, 84.9 mg, 0.5 mM) was dissolved in water and the solution was cooled to 0 °C in an ice bath; GSH (in a 1:4 molar ratio) was then added to form intermediates (Figure S1a). Second, NaOH was added to adjust the pH value (final pH ≈ 7) and to assist the dispersion of white precipitate (Figure S1 b). To be noted, the addition of NaOH is very important for the high-yield synthesis of silver nanoclusters. Without NaOH, a considerable amount of large nanoparticles (*ca.* 8~10 nm) was obtained. It was thus inferred that NaOH plays multiple roles in our successful synthesis: it could promote the dispersion of Ag-GSH complex, regulate the parameters of Ag-GSH complex aggregates (such as the size and structure) and tune the formation kinetics of silver nanoclusters by reducing the reduction ability of $NaBH_4$ and accelerating the etching ability of free glutathione.[23] Third, $NaBH_4$ (10-fold molar excess with respect to $AgNO_3$) in ice water was added drop by drop under vigorous stirring. The reaction solution slowly turned from light yellow to deep brown (Figure S1c and d), indicating the reduction of precursor and the formation of silver nanoclusters. After ageing for ~ 7 hours, the pure product was obtained by direct precipitation with excess methanol without extra purification process since the cluster product was mono-disperse. The mono-dispersity of the product was checked by polyacrylamide gel electrophoresis (PAGE) analysis. The initial product (1 hour after the addition of $NaBH_4$) shows two diffuse and broad bands in PAGE analysis: the first lies in brown purple and the second is bright-orange in visible light. With reaction time increasing, the purple band in the product gradually decreases and eventually disappears completely after ~7 hours and only the well-defined orange band (Figure 1A inset, and Figure S2) is observed in various conditions of PAGE operation (Figure S3), indicating a high purity of as-prepared product. The fact that recrystallization twice doesn't lead to changes of UV-Vis absorption and PAGE results further confirms the purity of the product (Figure 1B, inset d). It is important to note that the reaction can be readily scaled up (*e.g.*, by 10-fold, ~1 g clusters can be obtained, see Figure 1B inset c).. The high yield in this study is likely due to subtle tuning of reaction conditions (the control of pH value, the choice of solvent, the adequate prolongation of reaction time, *etc*). By carefully controlling the reaction kinetics and thermodynamics,[2,11a,24] a specific chemical environment could be attained leading to the formation of mono-sized silver nanoclusters.

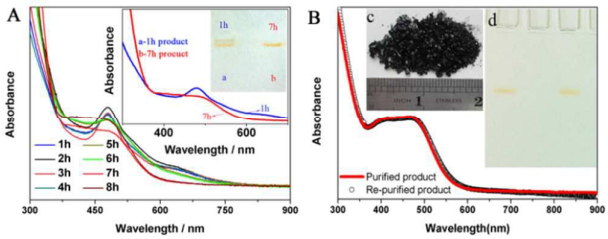

Fig. 1. A) UV-Vis absorption evolution with the extending of reaction time from 1h to 8h (recorded per hour). The peak at ~480 nm finally turns into the platform from ~374 nm to 485 nm. Inset, the UV-Vis absorption spectra and PAGE photos taken after 1 hour's (a) and 7 hours' (b) ageing. Note: the reaction mixture was characterized directly without any purification. B) UV-Vis absorption spectra of the as-prepared product and the further purified product (recrystallized for twice). Inset, (c) ~1 gram of Ag14(SG)11 pictured with a stainless ruler for scale (the product is about 1 inch in height and 2 inches in width); (d) PAGE analysis of the as-prepared product (left) and the further purified product (right) (recrystallized for twice).

For the as-purified silver nanoclustes we have firstly performed UV-vis absorption measurements and found that, instead of a plasmon band at ~450 nm known for silver nanoparticles (*e.g.*, larger than 3 nm), there displays a special absorption platform from 374 nm to 485 nm (Figure 1B), which is similar to those of recently reported clusters.[25] Mass spectrometry (MS) is well recognized as a powerful tool to identify metal nanoclusters, but comes across a challenge in determining the exact formula of silver clusters likely due to two facts. One is that silver itself has a complicated isotopic distribution; and the other is that the silver clusters are generally not as stable as gold nanoclusters. In striking contrast to numerous gold nanoclusters, only a couple of

mono-thiolated silver clusters were identified by isotope-resolved MS until now.[11-17] In this work we have paid great efforts endeavouring to improve the stability and purity of the analyte, until finally we succeeded in ESI-MS analysis of the intact silver clusters. The dominant peak was found at m/z 1625.1725 (Figure 2A) in the ESI-MS spectrum (acquired in the negative ion mode). The spacing of the isotope peaks was near 0.33 (Figure 2A inset) indicating that the ionized clusters bear a -3 charge (z), thus the m/z value of the peak represents one third of molecular ion mass, which matches with the theoretical mass of $[Ag_{14}(SG)_{11}\text{-}3H]^{3-}$ (1625.4945, deviation 0.3220), but doesn't match with the recently reported ESI data of $Ag_{35}(SG)_{18}$.[16c] Careful calculation reveals that the m/z value of the base peak matches better with the theoretical mass of $[Ag_{14}(SG)_{11}\text{-}4H]^{3-}$ (1625.1586, deviation 0.0139). Based on the high performance of the MS facility (error < 5 ppm at m/z = 1000, external calibration), the assignment for $[Ag_{14}(SG)_{11}\text{-}4H]^{3-}$ should be more accurate, and it is supported by the excellent agreement of the simulated and experimental isotopic distributions (Figure 2A inset).

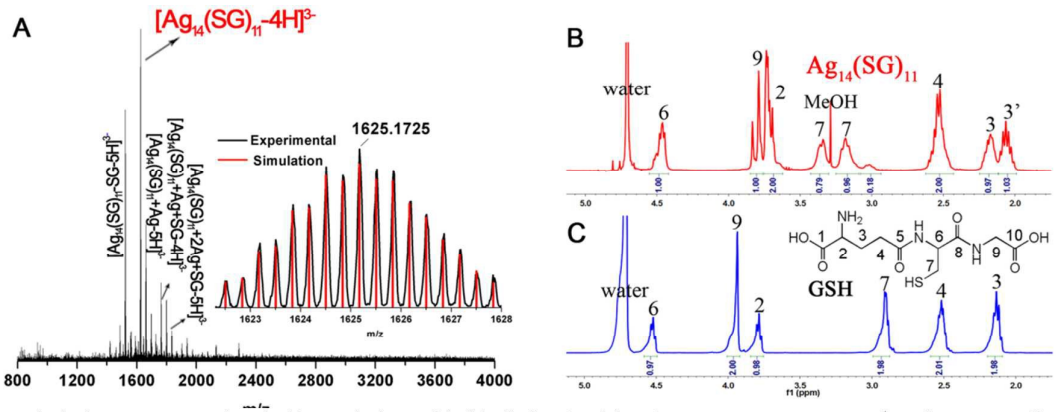

Fig. 2. Electrospray-ionization mass spectrum (acquired in negative ion mode) of the final product (A). Peaks at 1522, 1660, 1763, 1798 m/z are fragment or adducts with -3 charge state (see Supporting Information for more details). Inset A, shows the experimental (black) and simulated (red) isotopic patterns of $[Ag_{14}(SG)_{11}\text{-}4H]^{3-}$. NMR spectra of $Ag_{14}(SG)_{11}$ clusters (B) and free GSH (C). The carbon atoms in GSH were labled by the numbers 1-10, see inset in (C).

Besides the dominant peak in the mass spectrum, a few minor peaks at m/z 1522.8301, 1660.4990, *etc*. can also be observed in Figure 2A. These peaks are assigned to the fragments and adducts of the parent $[Ag_{14}(SG)_{11}\text{-}4H]^{3-}$ (abbreviated as M^{3-}). Among them, the peak at m/z 1522.8301 can be well assigned to the fragment $[Ag_{14}(SG)_{11}\text{-SG-}5H]^{3-}$ ($[M\text{-GSH}]^{3-}$, deviation: 0.0329) after one ligand in the parent ion was lost; the peak at m/z 1660.4990 corresponds to the adduct $[Ag_{14}(SG)_{11}\text{-}5H\text{+}Ag]^{3-}$ ($[M\text{+Ag-H}]^{3-}$, deviation: 0.0415) after one silver ion was adsorbed on $[Ag_{14}(SG)_{11}\text{-}4H]^{3-}$, *etc*. It is worth mentioning that the multiple PAGE analysis in various conditions (Figure S3) confirmed the mono-dispersity of the product; and the further purification of the as-prepared product doesn't lead to the characterization difference by UV/Vis/NIR spectroscopy and PAGE (Figure 1B). Furthermore, the excellent agreement between the experimental and simulated isotope patterns provides strong support for the assignments (for details see Figure S4). Also inductively coupled plasma-atomic emission spectrometry (ICP-AES) provides another evidence. The measured content of silver in the sample is 29.5% (± 1.6%), close to the expected value for $Ag_{14}(SG)_{11}$. Finally, X-ray photoelectron spectroscopy (XPS) analysis further provides support: the Ag/S atomic ratio revealed by quantitative measurement is 1.26 (±0.03):1, in excellent agreement with the composition of $[Ag_{14}(SG)_{11}\text{-}4H]^{3-}$ (expected Ag/S atomic ratio: 1.27:1), but deviated from the composition of $[Ag_{14}(SG)_{10}\text{-}4H]^{3-}$ (expected Ag/S atomic ratio: 1.40:1) or $[Ag_{15}(SG)_{11}\text{-}4H]^{3-}$ (expected Ag/S atomic ratio: 1.36:1). It can thus be concluded that the nanocluster product is composed of 14 silver atoms and 11 glutathione ligands.

Following the determination of formula of the Ag_{14} nanocluster, an interesting question pertains to the atomic packing structure adopted in the Ag_{14} core. Single crystal parsing is known as a reliable approach to determine chemical structures, however as a matter of fact, it is still a challenge to grow high-quality single crystals of mono-thiolated silver clusters (despite a success of Ag_{44} (*p*-MBA)$_{30}$).[10] Similar compounds analogy is helpful to ascertain the structures of chemicals, but severl reported silver nanoparticles including Ag_{16},[26a] Ag_{32},[26a] Ag_{62},[26b,c] Ag_{70},[26d] Ag_{262},[26d] Ag_{320},[26e] and Ag_{490}[26e] are not mono-thiolated, and even the recently reported $Ag_{14}(SC_6H_3F_2)_{12}(PPh_3)_8$[27] is also not really appliable since its composition largely differs from that of $Ag_{14}(SG)_{11}$. Therefore, it is highly desirable to probe the structure of Ag_{14} nanocluster by other means, in particular, to confirm whether its staple motif is similar to that of Au_{25}[4] and Ag_{44}.[10] Previously, we have successfully concluded the existence of $Au_2(SG)_3$ surfaces in glutathione-protected Au_{25} clusters.[28] Herein, NMR was employed to determine the type of the staple motif of Ag_{14}. The 1D NMR spectrum of Ag_{14} is shown in Figure 2B, as a comparison, the 1D NMR spectrum of pure glutathione is also presented. The splitting of H-7 is expected due to the induction of chiral carbon-6 and the revolving restriction of C-S bond after the formation of Au-S bond, however, this was not observed in gold nanoclusters[28] for the obvious splitting of proton 3 and slight splitting of proton 4, ascribing to that the adjacent amine group strongly adsorbs on

silver core. Interestingly, overlapped multiple peaks are found in the chemical shift ranging from 3.6 ppm to 3.9 ppm in the 1D NMR spectrum of Ag_{14}. The combination of homonuclear correlation spectroscopy (COSY) and heteronuclear single quantum correlation (HSQC) reveals that it is due to the quadruplication of proton-9 signal, indicating that the adjacent –NH– and –COOH groups have interactions with proton-9 (2D NMR details in Figure S6). Such a phenomenon was also not observed in the NMR spectrum of gold nanocluster.[28] To probe the staple motif of Ag_{14}, H-7 is the focus of attention due to it is adjacent to Ag-S binding. The 1D NMR spectrum, together with 2D COSY and HSQC demonstrates that there is no other splitting of proton 7 except the chiral splits, different from the case of Au_{25},[28] excluding the possible binding mode of $–[GS_1–Ag–SG_2–Ag–SG_1]–$ which would result in two pairs of H-7 peaks at 2:1 ratio. The novel staple type $Ag_2(SR)_5$ previously found in Ag_{44} is also excluded in this study as it will lead to three pairs of peaks at 1:2:2 ratio; other staple types like $Ag_n(SR)_{n+1}$ ($n > 3$) take even smaller possibility because all of them will produce splits distinctly different from the experimental results in this work. The most reasonable situation is that dominant $–[GS_1–Ag–S_1G]–$ staple motifs are adopted.[16b]

The fluorescence of silver nanoparticles[29] has long been an intriguing topic due to their potential application in sensing and bioimaging, *etc*. Although highly fluorescent silver nanoclusters protected by macromolecules (DNA, dendrimers, peptides, *etc*.) have been extensively studied,[30] highly fluorescent silver nanoclusters protected by small molecules challenge facile synthesis procedures. Previously reported studies revealed that both the ligands and the surface charge on the metal core play pivotal role in the emission of thiolated gold nanoclusters,[22] but the lack of understanding of the fluorescence fundamentals could be a key challenging the design of efficient protocols to synthesize highly fluorescent metal nanoclusters. Herein, it is revealed that Ag_{14} shows obvious fluorescence with UV irradiation, as shown in Figure 3. When excited at 400 nm, it exhibits a maximum emission at 640 nm with a large Stock shift. Further experiments reveal that both the emission intensity and the emission maximum wavelength are not influenced by the excitation wavelength in the range of 400-490 nm, indicating the high purity and stability of Ag_{14} nanoclusters. To be noted, both GSH and Ag-SG show no obvious fluorescence in the same conditions, and the excitation spectrum resembles the absorption spectrum (for a comparison, see Figure S7)**.** The fluorescence lifetimes were determined to be 0.32 ns (± 0.02 ns， 48.24%) and 2.72 ns (±0.14 ns,51.76%), as addressed in Figure S8. Also provided investigation is salt effect on the fluorescence of the cluster (see Figure S9)**.** Note that with the concentration of NaCl increased to 9.0 g/L, the fluorescence of Ag_{14} is quenched by 26.7% with the maximum emission redshifted for ~10 nm. Further lengthening the incubation time to 24 hours, another 9.9% decrease of fluorescence intensity was noted, indicating that the fluorescence of the cluster is not essentially influenced by the presence of salt. Ag_{14} shows high thermal stability in solid, and doesn't discompose until ~ 200 °C, see Figure S10.

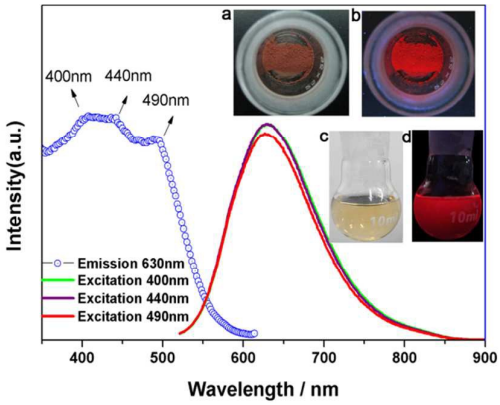

Fig. 3. Emission and excitation spectra of Ag_{14}. Inset, photographs of the clusters in solid (or solution) irradiated by UV (b, d) or visible light (a, c).

Ag_{14} can't well disperse in non-aqueous solvents, however, with the assistance of cetyltrimethyl ammonium bromide (CTAB), it can dissolve in alcohol (including methanol, ethanol, *n*-propanol and *n*-butyl alcohol), and it is found that the fluorescence intensity increases with the decrease of solvent polarity or dielectric constant (see Figure S11)[31] that is, the highest fluorescence intensity is achieved in *n*-butyl alcohol (dielectric constant: 17.8), and the lowest fluorescence intensity is acquired in methanol (dielectric constant: 33.0). On the other hand, the maximum emission wavelength redshifts with the decrease of solvent dielectric constant from methanol to ethanol, then to *n*-propanol (*n*-butyl alcohol is an except, see Figure S11). One possible reason to explain the solvent effect of the fluorescence intensity of Ag_{14} is the rigidity variety of the nanocluster surface in different solvents (the hydrophilic surface ligand becomes rigid in non-polar environment): with the decrease of solvent polarity, the surface rigidity of Ag_{14} increases, leading to the decrease of non-radiative transition and the increase of the fluorescence intensity as a result.[31c,d] Considering that the fluorescence intensity of Ag_{14} is dependent on the polarity of medium, we deem that the fluorescence intensity of Ag_{14} in cell is even higher than that in water, and speculate that the silver nanoclusters could label the cell for imaging. A549 cells, adenocarcinomic human alveolar basal epithelial cells, were used to investigate the intracellular location of Ag_{14}. As results, bright red fluorescence was observed in the living cells under the one-photon excited confocal microscopy (see details in Supporting Information, Figure S12), in strong contrast to the case without the labeling agent (Figure S13). It should be noted that the as-prepared nanoclusters accumulated in the cancer cells bear no surface modification or conjugation,[32,33] revealing that Ag_{14} has good penetrability in A549 cells. Two reasons likely explain the good penetrability of Ag_{14}: one is due to the ultrasmall size (~1nm) which reduces the spatial hindrance from the cell membrane compared with big particles, and the other is that the unique physicochemical properties of surface small molecule benefits the penetration

of Ag_{14} through cell membrane.[33] These two merits may also do good to the transportation of Ag_{14} in living cells. Confocal microscopy shows uniform fluorescence intensity inside the living cells, indicating that Ag_{14} not only stain the cell surface, but also well disperse inside the cell (including the cytoplasm and nucleus). Internalization of the $Ag_{14}(SG)_{11}$ silver clusters in living cells indicates potential applications not only in labeling cells to investigate extracellular dynamics but also in carrying drugs for cancer therapy. It is worth noting that although Ag_{14} can well disperse in A549 cells, it can aggregrate outside human-hamster hybrid (A(L)) cells (see Figure S14), indicating some specificity of Ag_{14} toward cell imaging. Here we emphasize on the cytotoxicity of the Ag_{14} nanoclusters in A549 cells, evaluated by using a 5-dimethylthiazol-2-yl-2,5-diphenyltetrazolium bromide (MTT) colorimetry method. Figure 4 shows the viability of cells labeled with five different concentrations of Ag_{14} clusters (0, 12.5, 25, 50, and 100 μg/ml) compared with the results of $AgNO_3$, GSH, Ag-GSH complex, and 8 nm silver nanoparticles by using the same manner and incubated at 37 °C. After 24 hours incubation, cell viability was still ca. 98% (± 7.9%) in high Ag_{14} concentration up to 100 μg/ml, which indicates the very low cytotoxicity of Ag_{14} nanoclusters.

It is well known that silver nanoparticles and silver ions are toxic due to their oxidation ability and/or relative large electron affinity.[34-37] Systematic investigations of the cytotoxicity for different silver species including Ag_{14}, $AgNO_3$, Ag-GSH complex, and 8 nm silver nanoparticles have also been done in this study, for the results, see Figure 4e. In order to better understand the low cytotoxicity of Ag_{14} nanoclusters, we need to emphasize that the biocompatible glutathione doesn't exhibit cytotoxicity, and experimental results indicate that Ag-GSH complex doesn't show obvious cytotoxicity with the concentrations up to 0.572 mmol/L due to the stability of silver ions by glutathione. Therefore it is reasonable that the glutathionate-protected Ag_{14} nanoclusters doesn't show obvious cytotoxicity even in higher concentration (200 μg/ml, *i.e.* 0.572 mmol/L on silver atom basis). The reason why large-sized silver nanoparticles are toxic probably imputes to two facts:[37] one is lower S/Ag atomic ratio (*e.g.*, 1:3 for ~8 nm nanoparticles vs. 11:14 for the Ag_{14} nanoclusters) allowing toxic redundant/released silver ions to interact with cells, the other is the stronger oxidation ability of large nanoparticles compared with the small silver clusters (a comparison of Ag3d binding energies for 8-nm nanoparticles and Ag_{14} nanoclusters is provided in Supporting Information, Figure S16).[38] It is extremely meaningful to investigate the possibility of silver nanoclusters as viable alternatives to state-of-the-art labeling materials in terms of cytoxicity and photobleaching lifetime. Figure S17 shows the cytotoxicity comparisons of Ag_{14} nanoclusters with CdTe/ZnTe [39a] and CdSe quantum dots,[39b] and distinctly demonstrates that Ag_{14} is less toxic than the investigated quantum dots. The photobleaching lifetime comparison between Ag_{14} and Hochst 33342 and Acridine orange (see Figure S18) also shows that Ag_{14} is of better performance than the widely used organic fluorophores in terms of photobleaching lifetime.[40] Taken together, these facts unambiguously suggest that the as-prepared silver nanoclusters is of potential biomedical applications.

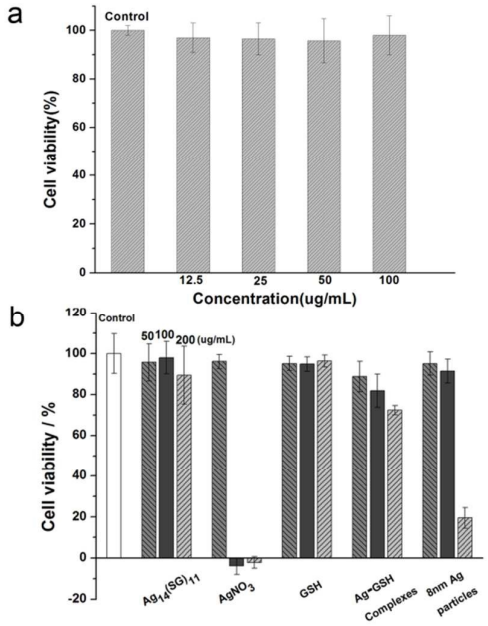

Fig. 4. (a) Viability of A549 cells at various concentrations of Ag_{14}; (b) A comparison of the viability of A549 cells in Ag_{14}, $AgNO_3$, GSH, Ag-GSH complex, and 8 nm silver nanoparticles. The concentrations of Ag_{14} is 50 ug/ml(left), 100 ug/ml(middle), 200 ug/ml(right), respectively. For $AgNO_3$, Ag-GSH complex and 8 nm silver nanoparticles, the silver atom molar concentrations in every species are same to those of Ag_{14} from left to right pillar, respectively; For GSH, the molar concentrations was adjusted to the same with those of glutathione ligand in Ag_{14} from left to right pillar, respectively.

In summary, a silver nanocluster Ag_{14} was synthesized by a one-pot one-cluster fashion after subtly tuning the reaction kinetics and thermodynamics. The nanocluster composition was determined by isotope-resolved ESI-MS combined with other analyses, and the structure was probed by 1D NMR spectrum together with 2D COSY and HSQC. The fluorescence properties of Ag_{14} were also investigated, pertaining to the medium-dependent emission intensity. Importantly, Ag_{14} was successfully applied to lung cancer (A549) imaging, representing for the first time to image cells labeled with small-molecule-protected silver nanoclusters. Furthermore, it was found that Ag_{14} nanoclusters have low cytotoxicity compared with some other silver species (including silver salt, silver complex and large silver nanoparticles), and the explanation was provided. The comparisons of silver nanoclusters to state-of-the-art labeling materials in terms of cytoxicity and photobleaching lifetime were also conducted. The multiple merits such as facile synthesis, red-emission, favorable penetrability, ultrasmall size, good biocompatibility and long photobleaching lifetime make Ag_{14} very promising for a wide range of potential applications.

Notes and references

1 a) A. C. Templeton, W. P. Wuelfing, R. W. Murray, *Acc. Chem. Res.* 2000, **33**, 27; b) R. Jin, *Nanoscale* 2010, **2**, 343; c) H. Häkkinen, *Nat. Chem.* 2012, **4**, 443; d) Y. Lu, W. Chen, *Chem. Soc. Rev.* 2012, **41**, 3594; e) Z. Luo, K.

Zheng, J. Xie, *Chem. Commun.* 2014, **50**, 5143; f) H. Xu, K. S. Suslick, *Adv. Mater.* 2010, **22**, 1078.
2 Z. Wu, M. A. MacDonald, J. Chen, P. Zhang, R. Jin, *J. Am. Chem. Soc.* 2011, **133**, 9670.
3 A. Das, T. Li, K. Nobusada, Q. Zeng, N. L. Rosi, R. Jin, *J. Am. Chem. Soc.* 2012, **134**, 20286.
4 a) Y. Shichibu, Y. Negishi, T. Tsukuda, T. Teranishi, *J. Am. Chem. Soc.* 2005, **127**, 13464; b) M. W. Heaven, A. Dass, P. S. White, K. M. Holt, R. W. Murray, *J. Am. Chem. Soc.* 2008, **130**, 3754; c) M. Zhu; C. M. Aikens, F. J. Hollander, G. C. Schatz, R. Jin, *J. Am. Chem. Soc.* 2008, **130**, 5883; d) Z. Wu, J. Chen, R. Jin, *Adv. Funct. Mater.* 2011, **21**, 177.
5 a) P. R. Nimmala, A. Dass, *J. Am. Chem. Soc.* 2011, **133**, 9175; b) C. Zeng, H. Qian, T. Li, G. Li, N. L. Rosi, B. Yoon, R. N. Barnett, R. L. Whetten, U. Landman, R. Jin, *Angew. Chem.* 2012, **124**, 13291; *Angew. Chem. Int. Ed.* 2012, *51*, 13114.
6 N. K. Chaki, Y. Negishi, H. Tsunoyama, Y. Shichibu, T. Tsukuda, *J. Am. Chem. Soc.* 2008, **130**, 8608.
7 G. Schmid, *Chem. Soc. Rev.* 2008, **37**, 1909.
8 P. D. Jadzinsky, G. Calero, C. J. Ackerson, D. A. Bushnell, R. D. Kornberg, *Science* 2007*,* **318***,* 430.
9 H. Qian, R. Jin, *Nano Lett.* 2009, **9**, 4883.
10 A. Desireddy, B. E. Conn, J. Guo, B. Yoon, R. N. Barnett, B. M. Monahan, K. Kirschbaum, W. P. Griffith, R. L. Whetten, U. Landman, T. P. Bigioni, *Nature* 2013**, 501**, 399.
11 a) Z. Wu, E. Lanni, W. Chen, M. E. Bier, D. Ly, R. Jin, *J. Am. Chem. Soc.* 2009, **131**, 16672; b) T. Udayabhaskararao, Y. Sun, N. Goswami, S. K. Pal, K. Balasubramanian, T. Pradeep, *Angew. Chem.* 2012, **124**, 2197; *Angew. Chem. Int. Ed.* 2012, **51**, 2155.
12 Y. Sun, K. Balasubramanian, T. U. B. Rao, T. Pradeep, *J. Phys. Chem. C* 2011, **115**, 20380.
13 T. U. B. Rao, T. Pradeep, *Angew. Chem.* 2010, ***122***, 4017; *Angew. Chem. Int. Ed.* 2010, **49**, 3925.
14 T. U. B. Rao, B. Nataraju, T. Pradeep, *J. Am. Chem. Soc.* 2010, **132**, 16304.
15 X. Yuan, M. I. Setyawati, A. S. Tan, C. N. Ong, D. T. Leong, J. Xie, *NPG Asia Mater.* 2013, **5**, e39.
16 a) J. Guo, S. Kumar, M. Bolan, A. Desireddy, T. P. Bigioni, W. P. Griffith, *Anal. Chem.* 2012, **84**, 5304; b) T. Udayabhaskararao, M. S. Bootharaju, T. Pradeep, *Nanoscale* 2013, **5**, 9404; c) M. S. Bootharaju, V. M. Burlakov, T. M. D. Besong, C. P. Joshi, L. G. AbdulHalim, D. M. Black, R. L. Whetten, A. Goriely, O. M. Bakr, *Chem. Mater.* 2015, **27**, 4289.
17 a) O. M. Bakr, V. Amendola, C. M. Aikens, W. Wenseleers, R. Li, L. D. Negro, G. C. Schatz, F. Stellacci, *Angew. Chem.* 2009, **121**, 6035; *Angew. Chem. Int. Ed.* 2009, **48**, 5921; b) I. Chakraborty, W. Kurashige, K. Kanehira, L. Gell, H. Häkkinen, Y. Negishi, T. Pradeep, *J. Phys. Chem. Lett.* 2013, **4**, 3351; c) L. G. AbdulHalim, S. Ashraf, K. Katsiev, A. R. Kirmani, N. Kothalawala, D. H. Anjum, S. Abbas, A. Amassian, F. Stellacci, A. Dass, I. Hussain, O. M. Bakr, *J. Mater. Chem. A* 2013, **1**, 10148; d) K. M. Harkness, Y. Tang, A. Dass, J. Pan, N. Kothalawala,V.J. Reddy, D. E. Cliffel, B. Demeler, F. Stellacci, O. M. Bakr, J. A. McLean, *Nanoscale*, 2012, **4**, 4269.
18 a) C. I. Richards, S. Choi, J. -C. Hsiang, Y. Antoku, T. Vosch, A. Bongiorno, Y. -L. Tzeng, R. M. Dickson, *J. Am. Chem. Soc.* 2008, **130**, 5038; b) T. Zhou, Y. Huang, W. Li, Z. Cai, F. Luo, C. J. Yang, X. Chen, *Nanoscale* 2012, **4**, 5312; c) H. Xu, K. S. Suslick, *ACS Nano* 2010, **4**, 3209.
19 a) J. Yu, S. Choi, C. I. Richards, Y. Antoku, R. M. Dickson, *Photochem. Photobiol.* 2008, *84*, 1435; b) Y. W. Zhou, C. M. Li, Y. Liu, C. Z. Huang, *Analyst* 2013, **138**, 873; b) W. Guo, J. Yuan, Q. Dong,E. Wang, *J. Am. Chem. Soc.* 2010, **132**, 932; c) Y. Antoku, J. -I. Hotta, H. Mizuno, R. M. Dickson, J. Hofkens, T. Vosch, *Photochem. Photobiol. Sci*. 2010, **9**, 716; d) Z. Sun, Y. Wang, Y. Wei, R. Liu, H. Zhu, Y. Cui, Y. Zhao, X. Gao, *Chem. Commun.* 2011, **47**, 11960; e) S. Choi, J. Yu, S. A. Patel, Y. -L. Tzeng, R. M. Dickson, *Photochem. Photobiol. Sci.* 2011, **10**, 109; f) J. Yuan, W. Guo, E. Wang, *Anal. Chem. Acta,* 2011, **706**, 338.
20 C. Zhou, M. Long , Y. Qin , X. Sun , J. Zheng, *Angew. Chem.* 2011, ***123***, 3226; *Angew. Chem. Int. Ed.* 2011, **50**, 3168; b) H. S. Choi, W. Liu, P. Misra, E. Tanaka, J. P. Zimmer, B. I. Ipe, M. G. Bawendi, J. V. Frangioni, *Nat. Biotechnol.* 2007, **25**, 1165.
21 M. A. H. Muhammed, P. K. Verma, S. K. Pal, R. C. A. Kumar, S. Paul, R. V. Omkumar, T. Pradeep, *Chem. Eur. J.* 2009, **15**, 10110.
22 a) Z. Wu, R. Jin, *Nano Lett.* 2010, **10**, 2568; b) Z. Luo, X. Yuan, Y. Yu, Q. Zhang, D. T. Leong, J. Y. Lee, J. Xie, *J. Am. Chem. Soc.* 2012, **134**, 16662.
23 X. Yuan, B. Zhang, Z. Luo, Q. Yao, D. T. Leong, N. Yan, J. Xie, *Angew. Chem.* 2014, **126**, 4711; *Angew. Chem. Int. Ed.* 2014, **53**, 4623.
24 M. Zhu, E. Lanni, N. Garg, M. E. Bier, R. Jin, *J. Am. Chem. Soc.* 2008, **130**, 1138.
25 a) S. Kumar, M. D. Bolan, T. P. Bigioni, *J. Am. Chem. Soc.* 2010, **132**, 13141; b) F. Bertorelle, R. Hamouda, D. Rayane, M. Broyer, R. Antoine, P. Dugourd, L. Gell, A. Kulesza, R. Mitrić, V. Bonačić -Koutecký, *Nanoscale*, 2013, **5**, 5637; c) A. Baksi, M. S. Bootharaju, X. Chen, H. Hakkinen, T. Pradeep, *J. Phys. Chem. C* 2014, **118**, 21722.
26 a) H. Yang, Y. Wang, N. Zheng, *Nanoscale* 2013, **5**, 2674; b) G. Li, Z. Lei, Q. -M. Wang, *J. Am. Chem. Soc.* 2010, 132, 17678; c) S. Jin, S. Wang, Y. Song, M. Zhou, J. Zhong, J. Zhang, A. Xia, Y. Pei, M. Chen, P. Li, M. Zhu, *J. Am. Chem. Soc.* 2014, **136**, 15559; d) D. Fenske, C. Persau, S. Dehnen,C. E. Anson, *Angew. Chem.* 2004, **116**, 309; *Angew. Chem. Int. Ed.* 2004, **43**, 305; e) C. E. Anson, A. Eichhöfer, I. Issac, D. Fenske, O. Fuhr, P. Sevillano, C. Persau, D. Stalke,J. Zhang, *Angew. Chem.* 2008, **120**, 1346; *Angew. Chem. Int. Ed.* 2008, **47**, 1326.
27 H. Yang, J. Lei, B. Wu, Y. Wang, M. Zhou, A. Xia, L. Zheng, N. Zheng, *Chem. Commun.* 2013, **49**, 300.
28 Z. Wu, C. Gayathri, R. R. Gil, R. Jin, *J. Am. Chem. Soc.* 2009, **131**, 6535.
29 a) G. A. Ozin, S. A. Mitchell, *Angew. Chem.* 1983, **95**, 706; *Angew. Chem. Int. Ed.* 1983, **22**, 674; b) G. A. Ozin, F. Hugues, S. M. Mattar, D. F. McIntosh, *J. Phys. Chem.* 1983, **87**, 3445; c) W. Harbich, S. Fedrigo, F. Meyer, D. M. Lindsay, J. Lignieres, J. C. Rivoal, D. Kreisle, *J. Chem. Phys.* 1990, **93**, 8535.
30 a) S. Choi, R. M. Dickson, J. Yu, *Chem. Soc. Rev.* 2012, **41**, 1867; b) J. Zheng, R. M. Dickson, *J. Am. Chem. Soc.* 2002, **124***,* 13982; c) S. M. Copp, P. Bogdanov, M. Debord, A. Singh, E. Gwinn, *Adv. Mater.* 2014, **26**, 5839.
31 a) I. Díez, M. Pusa, S. Kulmala, H. Jiang, A. Walther, A. S. Goldmann, A. H. E. Müller, O. Ikkala, R. H. A. Ras, *Angew. Chem. Int . Ed.* 2009, **48**, 2122; b) I. Díez, H. Jiang, R. H. A. Ras, *Chem. Phys. Chem*. 2010, **11**, 3100; c) Y. Li, X. Wang, S. Xu, W. Xu, *Phys. Chem. Chem. Phys.* 2013, **15**, 2665; d) K. Pyo, V. D. Thanthirige, K. Kwak, P. Pandurangan, G. Ramakrishna, D. Lee, *J. Am. Chem. Soc.* 2015, **137**, 8244.
32 a) L. Polavarapu, M. Manna, Q. -H. Xu, *Nanoscale* 2011, **3**, 429; b) L. Shang, R. M. Dorlich, S. Brandholt, R.

Schneider, V. Trouillet, M. Bruns, D. Gerthsen, G. U. Nienhaus, *Nanoscale* 2011, **3**, 2009; c) X. -D. Zhang, Z. Luo, J. Chen, X. Shen, S. Song, Y. Sun, S. Fan, F. Fan, D. T. Leong, J. Xie, *Adv. Mater.* 2014, **26**, 4565; d) D. Chen, Z. Luo, N. Li, J. Y. Lee, J. Xie, J. Lu, *Adv. Funct. Mater.* 2013, **23**, 4324.

33 a) L. Yang, L. Shang, G. U. Nienhaus, *Nanoscale* 2013, **5**, 1537; b) K. Huang, H. Ma, J. Liu, S. Huo, A. Kumar, T. Wei, X. Zhang, S. Jin, Y. Gan, P. C. Wang, S. He, X. Zhang, X. -J. Liang, *ACS Nano* 2012, **6**, 4483; c) M. Zhu, G. Nie, H. Meng, T. Xia, A. Nel, Y. Zhao*, Acc. Chem. Res.* 2012*,* **46***,* 622.

34 a) H. J. Johnston, G. Hutchison, F. M. Christensen, S. Peters, S. Hankin, V. Stone, *Critical Reviews in Toxicology*, 2010, **40**, 328; b) W. -S. Cho, M. Cho, J. Jeong, M. Choi, H. -Y. Cho, B. S. Han, S. H. Kim, H. O. Kim, Y. T. Lim, B. H. Chung, J. Jeong, *Toxicol Appl Pharmacol* 2009, **236**, 16.

35 E. Hidalgo, C. Domínguez, *Toxicol. Lett.* 1998, **98**, 169.

36 P. V. AshaRani, G. L. K. Mun, M. P. Hande, S. Valiyaveettil, *ACS Nano* 2009, **3**, 279.

37 H. J. Johnston, G. Hutchison1, F. M. Christensen, S. Peters, S. Hankin, V. Stone1, *Critical Reviews in Toxicology*, 2010, **40**, 328.

38 M. Wang, Z. Wu, Z. Chu, J. Yang, C. Yao, , *Chem. Asian J.* 2014, **9**, 1006.

39 a) W. -C. Law, K. -T. Yong, I. Roy, H. Ding, R. Hu, W. Zhao, P. N. Prasad, *Small* 2009, **5**, 1302; b) L. M. Maestro, E. M. Rodríguez, F. S. Rodríguez, M. C. I. I. Cruz, A. Juarranz, R. Naccache, F. Vetrone, D. Jaque, J. A. Capobianco, J. G. Solé, *Nano Lett*. 2010, **10**, 5109.

40 X. Gao, L. Yang, J. A. Petros, F. F. Marshall, J. W. Simons, S. Nie, *Current Opinion in Biotechnology*, 2005, **16**, 63.

The table of contents

A fluorescent,bio-compatible silver cluster (Ag_{14}) is synthesized in a one-pot one-cluster fashion, and successfully applied to imaging living cells A549.